Korean J. Chem. Eng., **28**(4), 1120-1125 (2011)
DOI: 10.1007/s11814-010-0458-2

Formation of 1-D ZnTe nanocrystals by aerosol-assisted spray pyrolysis

Dae-Jin Kim*,‡, Jun-Woo Kim*, Eui Jung Kim, and Kee-Kahb Koo*,†**

*Department of Chemical and Biomolecular Engineering, Sogang University, Seoul 121-742, Korea
**Department of Chemical Engineering, University of Ulsan, Ulsan 680-749, Korea
(*Received 29 August 2010 • accepted 19 October 2010*)

Abstract−One-dimensional (1-D) ZnTe nanowires were prepared by aerosol-assisted spray pyrolysis using a mixture of ZnO (1 mmol)/OA (4 mL)/TOPO (0.8 g)/ODE (4 mL) as Zn precursor and Te/TOP (3 mL of 0.75 M) as Te precursor. The shape, size, and crystal structure of products were characterized by means of transmission electron microscope (TEM) and X-ray diffraction (XRD). The shape evolution of ZnTe nanocrystals from nanodots to nanowires was achieved by controlling the reaction temperature. ZnTe nanodots with average diameter of 8.3 nm were synthesized at 300 °C. "Earthworm-like" shaped ZnTe (linear ZnTe aggregates) consisting of primary ZnTe nanodots of about 16 nm in diameter were obtained at 400 °C. In addition, 1-D ZnTe nanowires were prepared at reaction temperature higher than 450 °C. Those experimental results suggest that ZnTe nanowires with zinc blende structure are formed from ZnTe nanodots by the oriented attachment due to insufficient surface capping of surfactant molecules and by strong dipole-dipole interaction of nanodots, followed by self-organization of linear aggregates at higher reaction temperatures. The linear ZnTe aggregates consisting of primary ZnTe nanodots may be an intermediate stage in the formation process of nanowires from nanodots.

Key words: ZnTe, Nanodots, Nanowires, Spray Pyrolysis

INTRODUCTION

Semiconductor nanocrystals are of great interest for both fundamental studies and their potential applications because their distinct optical and electronic properties are strongly dependent on their particle size and shape [1-4]. Therefore, control of the size and shape of semiconductor nanocrystals has been the most important issue in the synthesis of semiconductor nanocrystals in the past decades [5-8]. One-dimensional (1-D) semiconductor nanowires are of particular interest since they serve as key building blocks for the 'bottom-up' construction in the field of nanoscale electronic and photonic devices [9]. Among those semiconductor systems, the II-VI compound semiconductors such as CdSe, CdTe, and ZnSe have been widely studied due to their potential applications in solar cells, photodetectors, and light-emitting diodes (LEDs) [10-12]. Semiconductor nanowires can be prepared by various methods including the vapor-liquid-solid and solution-liquid-solid approaches, solvothermal methods, template-assisted growth, kinetic control of crystal growth direction, self-assembly, and thermolysis of a single source precursor in ligands [13,14].

Zinc telluride (ZnTe) is one of the most important semiconductor materials with a direct optical band gap of 2.26 eV at room temperature and a Bohr exciton radius of 6.2 nm [15,16]. It has potential applications in optoelectronic devices, such as green LEDs and solar cells [17,18], operating in the blue-green region of the spectrum and thermoelectric devices [19]. The crystal structure of ZnTe is very similar to that of CdSe or ZnSe, a commonly studied semiconductor [1,20,21]. However, size- and shape-controlled synthesis of ZnTe nanocrystals has received little attention compared with that of other chalcogenides such as CdSe, ZnSe, and PbSe. This may be due to the difficulty in production of ZnTe nanoparticles from a direct reaction between metal zinc and tellurium because zinc source is easily precipitated from the solution and elemental Te is not easily educed to Te anion [22]. The synthesis of spherical and rod-like shaped ZnTe nanocrystals by injecting a single molecular precursor ($[Zn(TePh)_2][TMEDA]$) into a mixed-surfactant solution was reported by Jun et al. [23]. They proposed a mechanism that the surfactants form rod-like micelles and they template the 1-D crystal growth. Recently, Yong et al. [24] synthesized ZnTe nanowires under a fixed moderated concentration of precursor: a mixture of ZnO (2 mmol)/phenyl ether (5 mL)/myristic acid (1.4 g)/dodecylamine (12 mmol) and trioctylphosphine tellurium (TOPTe, 2 mL of 0.75 M). Those ZnTe nanowires have an average diameter of 19 nm and typical lengths of more than 1 μm. Wang et al. [25] and Fanfair and Korgel [26] reported the synthesis of ZnTe nanowires using a solution-liquid-solid method. Bismuth (Bi) nanoparticles were used as seeds of 1D growth of ZnTe. ZnTe nanowires synthesized by the hydrogen-assisted thermal evaporation method in the presence of Au catalyst via the vapor-liquid-solid growth mechanism were also reported by Meng et al. [27]. However, to date, study on the formation of ZnTe nanowires is in an infant stage.

We have produced II-VI semiconductor nanoparticles including CdSe, CdTe, and ZnSe using aerosol-assisted spray pyrolysis [28,29]. Typically, nanostructured materials prepared by that method, including CdS, CdSe, CdTe, ZnS, ZnSe, MoS_2, NiO, TeO_2, $BaZrO_3$, Y_2O_3-ZrO_2, and $Ti_{1-x}Zr_xO_2$, have thermodynamically stable spherical shape [28-37]. In the present work, 1-D ZnTe nanowires prepared by controlling the reaction temperature are demonstrated, and their formation mechanism are discussed with temperature-depen-

†To whom correspondence should be addressed.
E-mail: koo@sogang.ac.kr
‡Present address: KCC Central Research Institute, Gyeonggi-do 446-912, Korea

dent results of experiments.

EXPERIMENTS

1. Materials

Zinc oxide (ZnO, 99.99%), tellurium powder (Te, 99.5%), tri-*n*-octylphosphine oxide (TOPO, tech. 90%), tri-*n*-octylphosphine (TOP, tech. 90%), oleic acid (OA, tech. 90%), and 1-octadecene (ODE, tech. 90%) were purchased from Sigma-Aldrich. Ethanol (99.5+%, HPLC grade) and toluene (99.5+%, HPLC grade) were from J. T. Baker. All chemicals were used as received without further purification.

2. Preparation of Zn Stock Solution

Zinc stock solution was prepared by mixing 1 mmol of ZnO, 4 mL of OA, 0.8 g of TOPO, and 4 mL of ODE under argon, and then heating the mixture to flask to 330 ºC in a three-neck flask under argon and cooled to room temperature.

3. Preparation of Te Stock Solution

0.75 M stock solution of TOPTe was prepared in advance. Typically, this was prepared by mixing 37.5 mmol (4.785 g) of Te powder with 50 mL of TOP under argon, and then heating the mixture to 250 ºC for 6 hours until the tellurium was completely dissolved. The resulting transparent yellow solution was cooled to room temperature and kept under argon for subsequent use in the synthesis.

4. Preparation of ZnTe Nanocrystals

Fig. 1 represents the experimental setup for aerosol-assisted spray pyrolysis consisting of an ultrasonic nebulizer (1.7 MHz), a furnace with an 80 cm long quartz tube reactor with a 2.8 cm diameter and the heating length is 50 cm, and a bubbler for collection of nanocrystals produced. The tube reactor was vertically equipped to prevent additional reaction by condensation of reactant solution. In a typical experiment, Zn stock solution and 3 mL of Te stock solution were diluted with addition of 30 mL of toluene at room temperature and then ultrasonically nebulized into microdroplets. The dense mist produced was carried by argon gas (1 L/min) through a quartz tube in a tube furnace kept at 400 ºC, where solvent evaporation and precursor reaction occurs and ZnTe nanocrystals are produced. ZnTe nanocrystals formed in the reaction tube were collected in a toluene-filled bubbler. Finally, ZnTe nanocrystals were precipitated with ethanol (30 mL) and isolated by centrifugation and decantation.

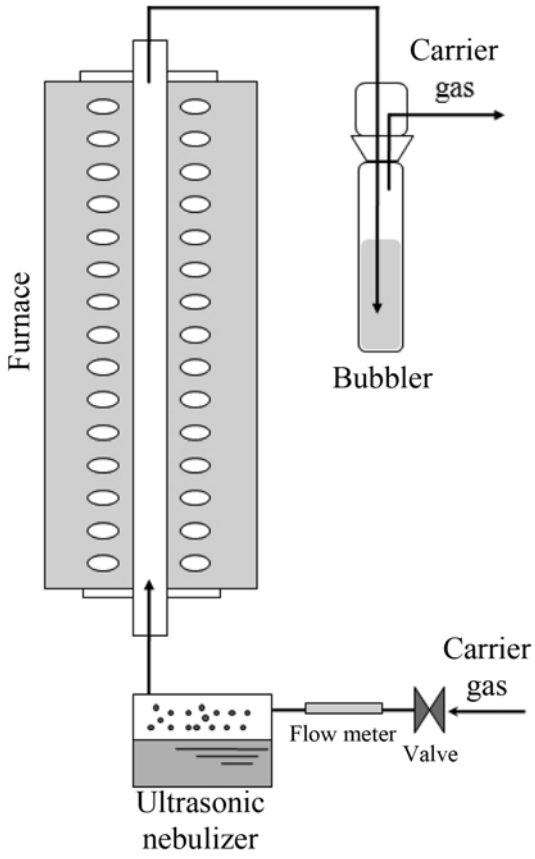

Fig. 1. Experimental setup for an aerosol-assisted spray pyrolysis system.

5. Characterization

Powder X-ray diffraction (XRD) patterns were measured using a Rigaku MiniFlex X-ray diffractometer operated at 30 kV and 15 mA with graphite-monochromatized Cu Kα radiation (λ=1.5418 Å). The scanning rate was 1.0 deg/min. Samples were prepared by washing with ethanol and dried under vacuum. A JEOL JEM-2100F field emission transmission electron microscope (TEM) operating at 200 kV was used to obtain images of ZnTe nanocrystals. Samples for TEM were prepared by putting a drop of toluene diluted solution of semiconductor nanocrystals onto an amorphous carbon substrate supported on a copper grid and then allowing the solvent to evaporate at room temperature. The elemental composition of the samples was analyzed using a HITACHI S-4300 scanning electron field emission microscope with X-ray energy-dispersed spectrometry (EDX) that is performed with precipitated ZnTe nanocrystals from bubbler.

RESULTS AND DISCUSSION

1-D ZnTe nanowires as well as zero-dimensional (0-D) ZnTe nanodots were produced by controlling reaction temperature ranging from 300 to 500 ºC in a moderated concentration of precursor: a mixture of ZnO (1 mmol)/OA (4 mL)/TOPO (0.8 g)/ODE (4 mL) as Zn precursor and Te/TOP (3 mL of 0.75 M) as Te precursor. The surfactant molecules with suitable chain lengths should be considered since they affect both nucleation and growth of nanocrystals. Preparation of the liquid state of precursor solution is especially essential to obtain nanocrystals in the present system, because the precursor solution should transfer as mist to a reactor at room temperature. In general, short chain length carboxylic acids like lauric acid ($C_{12}H_{24}O_2$) [38] and myristic acid ($C_{14}H_6O_2$) [24] are more effective ofr dissolving ZnO than long chain length carboxylic acids like oleic acid since those smaller ligands can be readily coordinated to Zn ion. However, as described in our previous work on formation of ZnSe nanospheres [29], the use of organic molecules for the dissolution of ZnO is very limited in aerosol-assisted spray pyrolysis because Zn stock solutions with short chain length ligands are solidified as their temperature is decreased to room temperature. Therefore, TOPO as a coordinating surfactant and ODE as a non-coordinating surfactant were employed, respectively, to achieve complete dissolution of the ZnO precursor. Synthesis of ZnTe should not differ much from that of ZnSe due to the similarity of the organometallic

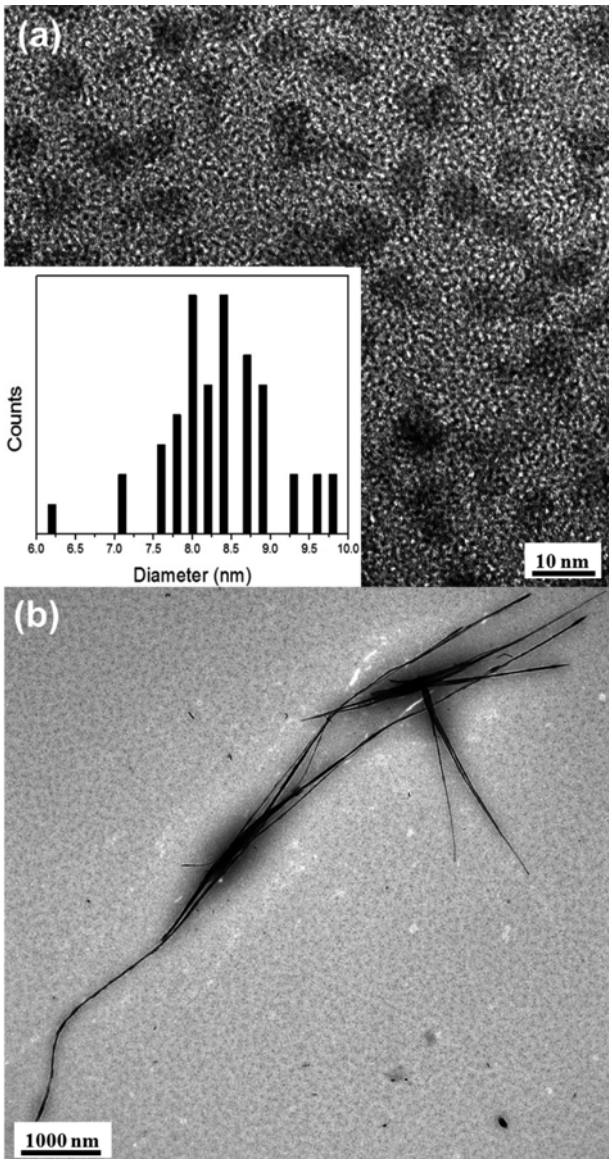

Fig. 2. TEM images of ZnTe nanocrystals: (a) ZnTe nanodots prepared at 300 °C and their size distribution (inset), (b) ZnTe nanowires prepared at 450 °C.

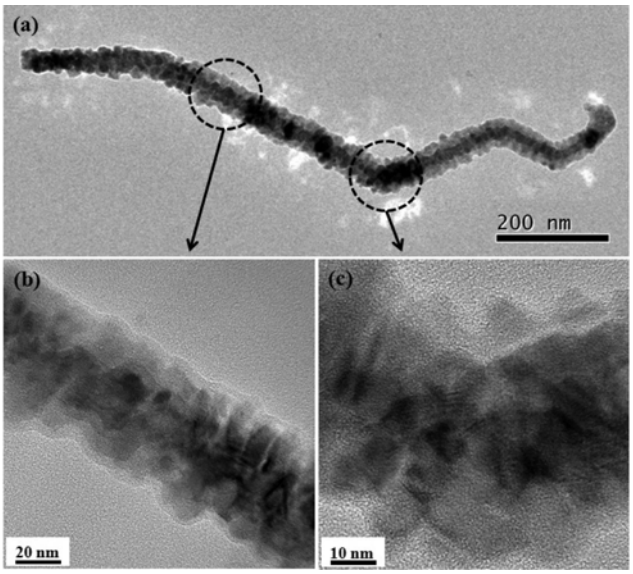

Fig. 3. TEM images of ZnTe nanoparticles prepared at 400 °C: (a) low-magnification TEM image, (b), (c) high-magnification TEM images.

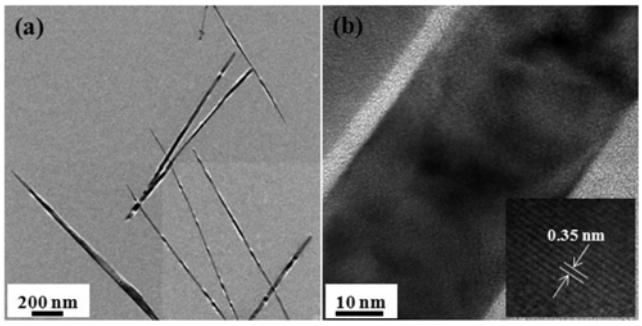

Fig. 4. TEM images of ZnTe nanocrystals prepared at 500 °C: (a) low-magnification TEM image, (b) high-magnification and high-resolution TEM images.

precursors; thus the precursor solutions and the experimental conditions are similar to those of ZnSe [29].

The shape and size of ZnTe nanocrystals prepared in the present work were found to be dramatically affected by the reaction temperature. Fig. 2(a) shows TEM image of ZnTe nanodots obtained at 300 °C and their size distribution. The average diameter of ZnTe nanodots calculated from TEM image is 8.3 nm and its standard deviation (σ) is 0.7.

It is noted that "earthworm-like" shaped ZnTe nanoparticles (linear ZnTe aggregates) are formed at 400 °C as shown in Fig. 3. High-magnification TEM images show that linear ZnTe aggregates obtained at 400 °C consist of primary ZnTe nanodots. Average diameter of primary ZnTe nanodots calculated from high-magnification TEM image of Fig. 3(c) is approximately 16 nm. We think those linear ZnTe aggregates seem to be an intermediate stage in the formation of nanowires from primary spherical nanodots. This linear aggregation of primary nanodots may be explained by oriented attachment and insufficient surface capping of surfactant molecules acting as a surface stabilizer, which may lead to increase in dipole-dipole interactions between primary nanodots [7,39-41].

On the other hand, 1-D ZnTe nanowires were found to be synthesized at higher reaction temperature. Figs. 2(b) and 4 show the TEM images of ZnTe nanowires prepared at 450 and 500 °C, respectively. The wires obtained at 450 °C are long and straight with diameter ranging from 20 to 35 nm and aspect ratio ranging from 120 to 250, as can be seen from Fig. 2(b). The length of nanowires is typically longer than 2 μm, and the longest one as can be seen from Fig. 2(b) is 7.6 μm.

When ZnTe was synthesized at 500 °C, smooth and straight nanowires, with an average diameter of 21 nm and aspect ratio of 65 to 140, were produced as shown in Fig. 4(a). Fig. 4(b) shows high-magnification and high-resolution images of crystalline ZnTe nanowires. The lattice fringe spacing is 0.35 nm, which corresponds to the (111) lattice planes of cubic structure of ZnTe.

Powder XRD diffraction measurements were conducted to exam-

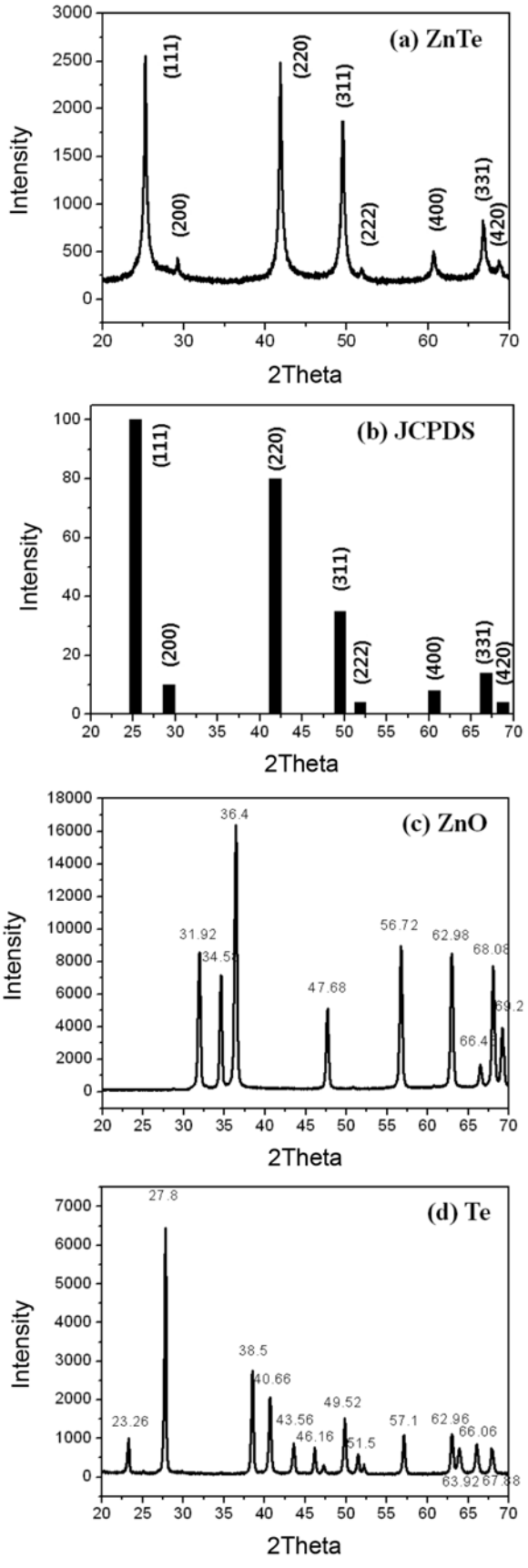

Fig. 5. Powder XRD patterns of (a) ZnTe nanoparticles prepared at 400 °C, (b) JCPDS No. 15-0746 (zinc blende structure of ZnTe), (c) ZnO powder, and (d) Te powder.

ine the crystal structure of ZnTe nanocrystals and their purity. In the present experiments, all ZnTe nanocrystals synthesized in the present work have zinc blende lattice structure. Fig. 5(a) shows that XRD pattern of ZnTe nanoparticles obtained at 400 °C and the positions of all diffraction peaks match well with the standard powder diffraction data of zinc blende (Joint Committee for Powder Diffraction Studies (JCPDS) No. 15-0746, Fig. 5(b)). The diffraction peaks at 25.24°, 29.92°, 41.84°, 49.52°, 51.88°, 60.66°, 66.72°, and 68.80° of ZnTe nanocrystals could be indexed to the (111), (200), (220), (311), (222), (400), (331), and (420) planes of the cubic-phase ZnTe with a crystal constant of a=6.103 Å. The powder XRD patterns of ZnO and Te powder were also examined to investigate the presence of unreacted precursors in final products (Fig. 5(c) and 5(d)). The absence of crystalline peaks of ZnO, Te, and others in the XRD pattern clearly indicates that those chemicals are dissolved completely in a precursor solution and the as-synthesized ZnTe nanocrystals are highly pure. On the basis of the full width at half-maximum (FWHM) of ZnTe (111) diffraction peak, the average diameter of the primary nanodots was calculated using Scherrer's formula: $D=(0.9\lambda)/(B\cos\theta)$, where D is the average diameter of nanocrystals, λ is the wavelength of the X-ray used, B is the full width in radians at half-maximum of the peak, and θ is the Bragg angle of the X-ray diffraction peak. The calculated value for the average diameter of the primary nanodots with the (111) peak at 2θ=25.24° is 16.2 nm, which agrees with the value of about 16 nm obtained from TEM results as shown in Fig. 3(c).

The composition of the ZnTe nanocrystals obtained at 400 °C was also analyzed by EDX (Fig. 6). The EDX pattern clearly confirms the presence of Zn and Te, and the atomic ratio of Zn : Te is 1 : 1.06 which is in agreement with stoichiometry of ZnTe. The presence of peaks for oxygen, carbon, and phosphorus in the EDX spectrum indicates that the residual chemicals such as OA and TOPO are bound around the surface of ZnTe nanocrystals.

In general, there are three key parameters for anisotropic growth of nanocrystals in solution-based routes: crystal structure of nanocrystals, monomer concentration in solution, and ability of surfactant molecules in growth stage of crystal. First, when the nanocrystals have a highly symmetric crystal structure such as zinc blende structure, faceted crystals with no unique growth direction have been reported to be produced [42]. On the other hand, when the nanocrystals have a lower symmetry structure such as wurtzite structure, anisotropic growth tends to occur [1,5,20]. Secondly, the anisotropic growth of nanocrystals occurs when there is a high concentration

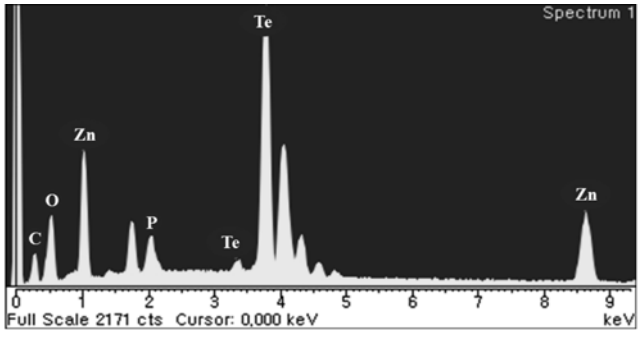

Fig. 6. EDX measurement of ZnTe nanocrystals prepared at 400 °C.

of monomer in solution [1]. Lastly, the significant surface energy differences between the various facets of nanocrystals and the selective adhesion of surfactant molecules on specific facets of nanocrystals make it possible to synthesize 1D semiconductor nanocrystals [43-45]. However, in the present work, the formation mechanism of 1D ZnTe nanocrystals differs from general growth mechanism mentioned above because 1D ZnTe nanocrystals with highly symmetric zinc blende structure were obtained at low monomer concentration. Recently, other anisotropic growth mechanism, which is oriented attachment, of semiconductor nanocrystals including CdSe [7], CdTe [39], and ZnS [40] in solution-based routes without the addition of high monomer concentration, has been reported.

We found that the reaction temperature is the most important parameter to control the shape of ZnTe nanocrystals in a moderate concentration of precursor. From TEM images, the temporal shape evolution of the ZnTe nanocrystals can be described as follows: spherical nanocrystals which are thermodynamically stable are formed at low reaction temperature (300 ºC) due to the low concentration of monomers (Fig. 2(a)), and then, they are spontaneously aggregated and formed as linear aggregates as reaction temperature is elevated to 400 ºC (Fig. 3). This may be an intermediate step in the formation of nanowires from primary nanodots by oriented attachment and linear aggregation. The linear aggregation process is driven by strong surface energy of primary nanodots caused by insufficient surface capping of surfactant molecules and strong dipole-dipole interaction between primary nanodots [29,39]. In addition, zinc blende structure of ZnTe has higher surface energy than does wurtzite structure, leading to strong dipolar interactions [24,40]. Those interactions can lead to oriented attachment. As the temperature increases, ZnTe nanowires may be subsequently formed from intermediate step by self-organization at higher reaction temperature (Fig. 2(b) and 4). The mean diameter of ZnTe nanowires obtained at reaction temperatures of 450 and 500 ºC is about 20-35 nm, and the mean diameter of "earthworm-like" shaped ZnTe nanoparticles is about 43-60 nm. It seems that intra-diffusion and reordering of molecules occur in a nanoparticle at high reaction temperature; thus, smooth and thin ZnTe nanowires are formed. Schematic diagram given in Fig. 7 summarizes nucleation and growth mechanism of ZnTe nanowires by oriented attachment. ZnTe nuclei can be easily obtained under suitable synthetic conditions. Then, the nuclei grow to primary nanocrystals and linear aggregates are formed from primary nanocrystals by oriented attachment and linear aggregation. Finally, 1-D nanowires can be produced by self-organization processes such as intra-diffusion and reordering of molecules at higher reaction temperature.

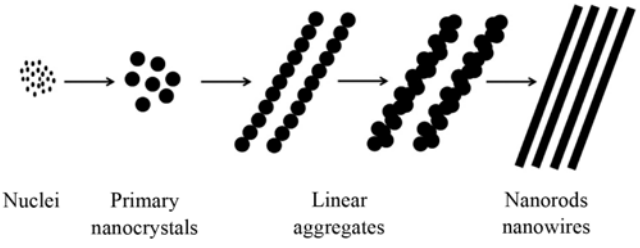

Fig. 7. Schematic illustrating the formation and shape evolution of zinc blende structure of ZnTe nanocrystals.

CONCLUSIONS

We have produced 1-D ZnTe nanowires by aerosol-assisted spray pyrolysis using a moderate mixture of ZnO (1 mmol)/OA (4 mL)/TOPO (0.8 g)/ODE (4 mL) as Zn precursor and Te/TOP (3 mL of 0.75 M) as Te precursor. From the observation of temperature-dependant results of experiments, the shapes of ZnTe nanoparticles are found to be significantly affected by reaction temperature in the present condition. We believe that 1-D ZnTe nanowires were formed from primary ZnTe nanodots by oriented attachment and linear aggregation and subsequent self-organization such as intra-diffusion and reordering at reaction temperature above 450 ºC. Those results suggest that the present method contributes to the production of 1-D semiconductor nanowires with a large-scale by continuous feeding of monomer precursors.

ACKNOWLEDGEMENT

This work was supported by the Sogang University Foundation Research Grant in 2009 and the Nano/Bio Science & Technology Program (M10536090001-05N3609-00110) of the Ministry of Education, Science and Technology (MEST).

NOMENCLATURE

LED : light-emitting diode
EDX : energy-dispersed spectrometry
FWHM : full width at half maximum
JCPDS : joint committee for powder diffraction studies
OA : oleic acid
ODE : 1-octadecene
TEM : transmission electron microscope
TOP : tri-*n*-octylphosphine
TOPO : tri-*n*-octylphosphine oxide
TOPTe : trioctylphosphine tellurium
XRD : X-ray diffraction
B : full width in radians at half-maximum of the peak [degree]
D : average diameter of nanocrystals [nm]
θ : Bragg angle of the X-ray diffraction peak [degree]
λ : wavelength of the X-ray used [nm]

REFERENCES

1. X. G. Peng, L. Manna, W. D. Yang, J. Wickham, E. Scher, A. Kadavanich and A. P. Alivisatos, *Nature*, **404**, 59 (2000).
2. X. Chen, A. Nazzal, D. Goorskey, M. Xiao, Z. A. Peng and X. G. Peng, *Phys. Rev.*, **B64**, 245304 (2001).
3. L. Manna, E. C. Scher and A. P. Alivisatos, *J. Clust. Sci.*, **13**, 521 (2002).
4. Y. W. Jun, J. W. Seo, S. J. Oh and J. Cheon, *Coord. Chem. Rev.*, **249**, 1766 (2005).
5. L. Manna, E. C. Scher and A. P. Alivisatos, *J. Am. Chem. Soc.*, **122**, 12700 (2000).
6. Z. A. Peng and X. G. Peng, *J. Am. Chem. Soc.*, **124**, 3343 (2002).
7. N. Pradhan, H. F. Xu and X. G. Peng, *Nano Lett.*, **6**, 720 (2006).
8. S. H. Lee, Y. J. Kim and J. Park, *Chem. Mater.*, **19**, 4670 (2007).
9. P. N. Prasad, *Nanophotonics*, Wiley-Interscience, New York (2004).

10. D. Xu, X. Shi, G. Guo, L. Gui and Y. Tang, *J. Phys. Chem.*, **B104**, 5061 (2000).
11. Q. Yang, K. Tang, C. Wang, Y. Qian and S. Zhang, *J. Phys. Chem.*, **B106**, 9227 (2002).
12. X. T. Zhang, Z. Liu, K. M. Ip, Y. P. Leung, Q. Li and S. K. Hark, *J. Appl. Phys.*, **95**, 5752 (2004).
13. Y. Wu and P. Yang, *J. Am. Chem. Soc.*, **123**, 3165 (2001).
14. B. L. Cushing, V. L. Kolesnichenko and C. J. O'Connor, *Chem. Rev.*, **104**, 3893 (2004).
15. T. Mahalingam, V. S. John, S. Rajendran and P. J. Sebastian, *Semicond. Sci. Technol.*, **17**, 465 (2002).
16. L. Li, Y. Yang, X. Huang, G. Li and L. Zhang, *J. Phys. Chem.*, **B109**, 12394 (2005).
17. B. L. Crowder, F. F. Morehead and P. R. Wagner, *Appl. Phys. Lett.*, **8**, 148 (1966).
18. S. Bhunia and D. N. Bose, *J. Cryst. Growth*, **186**, 535 (1998).
19. N. Mingo, *Appl. Phys. Lett.*, **85**, 5986 (2004).
20. Z. A. Peng and X. J. Peng, *J. Am. Chem. Soc.*, **123**, 1389 (2001).
21. L. Li, Q. S. Wu, Y. P. Ding and P. M. Wang, *Mater. Lett.*, **59**, 1623 (2005).
22. Y. Li, Y. Ding and Z. Wang, *Adv. Mater.*, **11**, 847 (1999).
23. Y. W. Jun, C. S. Choi and J. Cheon, *Chem. Commun.*, **101** (2001).
24. K.-T. Yong, Y. Sahoo, H. Zeng, M. T. Swihart, J. R. Minter and P. N. Prasad, *Chem. Mater.*, **19**, 4108 (2007).
25. F. Wang, A. Dong, J. Sun, R. Tang, H. Yu and W. E. Buhro, *Inorg. Chem.*, **45**, 7511 (2006).
26. D. D. Fanfair and B. A. Korgel, *Cryst. Growth Des.*, **8**, 3246 (2008).
27. Q. Meng, C. Jiang and S. X. Mao, *J. Cryst. Growth*, **310**, 4481 (2008).
28. D.-J. Kim, H. D. Jang, E. J. Kim and K.-K Koo, *Ultramicroscopy*, **108**, 1278 (2008).
29. D.-J. Kim and K.-K Koo, *Cryst. Growth Des.*, **9**, 1153 (2009).
30. K. Okuyama, I. W. Lenggoro, N. Tagami, S. Tamaki and N. Tohge, *J. Mater. Sci.*, **32**, 1229 (1997).
31. B. Xia, I. W. Lenggoro and K. Okuyama, *Adv. Mater.*, **13**, 1579 (2001).
32. Y. T. Didenko and K. S. Suslick, *J. Am. Chem. Soc.*, **127**, 12196 (2005).
33. S. E. Skrabalak and K. S. Suslick, *J. Am. Chem. Soc.*, **127**, 9990 (2005).
34. Y. Huang, Z. Zheng, Z. Ai, L. Zhang, X. Fan and Z. Zou, *J. Phys. Chem.*, **B110**, 19323 (2006).
35. H. Zhang and M. T. Swihart, *Chem. Mater.*, **19**, 1290 (2007).
36. M. M. Bucko and J. Oblakowski, *J. Eur. Ceram. Soc.*, **27**, 3625 (2007).
37. J. H. Bang, W. H. Suh and K. S. Suslick, *Chem. Mater.*, **20**, 4033 (2008).
38. H. S. Chen, B. Lo, J. Y. Hwang, G. Y. Chang, C. M. Chen, S. J. Tasi and S. J. J. Wang, *J. Phys. Chem.*, **B108**, 17119 (2004).
39. Z. Tang, N. A. Kotov and M. Giersig, *Science*, **297**, 237 (2002).
40. J. H. Yu, J. Joo, H. M. Park, S. I. Baik, Y. W. Kim, S. C. Kim and T. Hyeon, *J. Am. Chem. Soc.*, **127**, 5662 (2005).
41. E. J. H. Lee, C. Ribeiro, E. Longo and E. R. Leite, *J. Phys. Chem.*, **B109**, 20842 (2005).
42. S.-M. Lee, Y.-W. Jun, S.-N. Cho and J. Cheon, *J. Am. Chem. Soc.*, **124**, 11244 (2002).
43. S.-M. Lee, S.-N. Cho and J. Cheon, *Adv. Mater.*, **15**, 441 (2003).
44. W. W. Yu, Y. A. Wang and X. Peng, *Chem. Mater.*, **15**, 4300 (2003).
45. X. G. Peng, *Adv. Mater.*, **15**, 459 (2003).